Folding of Ubiquitin: A Simple Model Describes the Strange Kinetics

Sergei F. Chekmarev,*,† Sergei V. Krivov,‡ and Martin Karplus*,‡,§

Institute of Thermophysics, Siberian Branch of the Russian Academy of Sciences, Ac. Lavrent'ev av. 1, 630090 Novosibirsk, Russia, Laboratoire de Chimie Biophysique, ISIS, Université Louis Pasteur, Rue Blaise Pascal 4, 67000 Strasbourg, France, and Department of Chemistry and Chemical Biology, Harvard University, Cambridge, Massachusetts 02138

Received: November 23, 2005; In Final Form: March 12, 2006

The ubiquitin mutant Ub*G folding experiments of Sabelko et al. (*Proc. Natl. Acad. Sci. U.S.A.* **1999**, *96*, 6031−6036), in which "strange kinetics" were observed, are interpreted in terms of a simple kinetic model. A minimal set of states consisting of a semicompact globule, two off-pathway traps, and the native state are included; the fully unfolded state is not considered because folding to the semicompact globule is fast. Both the low- and the high-temperature experiments of Sabelko et al. are fitted by a system of kinetic equations determining the transitions between these states. It is possible that cold- and heat-denaturated states of Ub*G are the basis of the off-pathway traps. The fits of the kinetic model to the experimental results provides an estimate of the rate constants for the various reaction channels and show how their contributions vary with temperature. Introduction of an on-pathway intermediate instead of one of the off-pathway traps does not lead to agreement with the experiments.

I. Introduction

Recent progress in experimental studies of protein folding on millisecond and faster time scales has increased the interest in the existence and role of intermediates in the folding process.[1] Ubiquitin is a benchmark system for protein folding studies due to its structural and physical properties.[2] To provide a fluorescence probe for monitoring folding of ubiquitin, Khorasanizadeh et al.[3] replaced the largely buried Phe45 by Trp. In the recent experiments of Sabelko et al.,[4] which we analyze in this paper, a double mutant (F45W, V26G) of human ubiquitin (Ub*G) was used; the V26G mutation was added to destabilize core contacts and a critical helix to make cold denaturation possible.

In their temperature-jump experiments, Sabelko et al.[4] found that the time-dependent population of unfolded states varied with temperature from a double-exponential distribution at $T = 2$ °C to a stretched-exponential distribution at $T = 8$ °C. The interest in the latter is that it occurs on warming rather than cooling, in contrast to what is expected below the so-called glass transition.[5−6] Moreover, the high-temperature spectrum of characteristic times is (quasi-)continuous and spans a broad region, corresponding to what has been referred to as "strange kinetics".[7] In protein folding such kinetics have been associated with downhill folding through an array of intermediates separated by relatively low free energy barriers.[8−11] Sabelko et al.[4] adduced arguments in favor of a downhill folding scenario at $T = 8$ °C but also indicated that the kinetics at this temperature is well fitted by a three-exponential distribution. Thus, the presence of long-lived intermediates could not be ruled out.

Stretched-exponential distributions are convenient for approximation of experimental data, because they require just two parameters, a time constant and a power of the stretching exponent. A shortcoming of this approach is that the relation between the energy landscape and the parameters is not direct;[9−10] i.e., knowledge of the parameters gives little information about specific features of the landscape. Multiexponential distributions require more fitting parameters (twice the number of exponential terms). However, if these distributions are related to a specific model and represent solutions of a system of kinetic equations, then valuable insight into the folding process can be obtained. Recently, we simulated the Monte Carlo folding kinetics of a 27-bead square lattice protein model and showed that the results could be described by a simple kinetic model with off-pathway intermediates.[12] In this paper we use a similar model to interpret the data on Ub*G folding. We show that both the low- and the high-temperature experiments are well-described by a system of kinetic equations determining the transitions between characteristic states of the protein; in the minimal model, they are a semicompact globule, two off-pathway traps, and the native state. By comparing the theoretical solutions with the experimental results, we estimate the rate constants for the reaction channels and show how the significance of these channels varies with temperature. We also consider a model with an on-pathway intermediate, instead of one of the off-pathway traps, and show that this does not lead to agreement with the experimental results.

The paper is organized as follows. In section 2 we describe the kinetic schemes, and in section 3 we compare the theoretical solutions with experimental data and briefly discuss the results. Section 4 contains concluding remarks.

II. Kinetic model

We consider three kinetic schemes of the folding process; they are shown in Figure 1. The index "g" corresponds to a collapsed (semicompact globule) state, "d" to an off-pathway

* Authors to whom correspondence should be addressed. Phone: 33 388 416132/(617)495-4018 (M.K.); (383) 339-10-48 (S.F.C.). Fax: 33 388 608363/(617)496-3204 (M.K.); (383) 330-84-80 (S.F.C.). E-mail: marci@tammy.harvard.edu (M.K.); chekmarev@itp.nsc.ru (S.F.C.).

† Siberian Branch of the Russian Academy of Sciences.

‡ Université Louis Pasteur.

§ Harvard University.

10.1021/jp056799o CCC: $33.50
Published on Web 04/12/2006

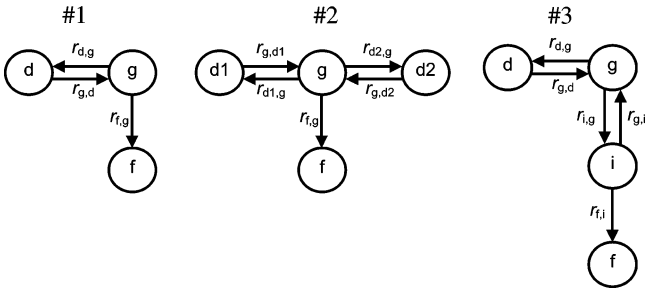

Figure 1. Kinetic schemes. Labels g, d, i, and f are for the semicompact globule, off-pathway and on-pathway intermediates, and native structure, respectively. Arrows show the directions of transitions.

intermediate ("dead-end trap"), "i" to an on-pathway intermediate, and "f" to the native state. Arrows show the directions of the transitions. Following the experimental conditions of ref 4, we do not include the fully extended (denaturted) state of the system; this would change the folding kinetics only at very short times (within the dead time of the experiments),[12] but the solution of kinetic equations would become considerably more complex. Since the experimental population of unfolded states[4] does not show a tendency to stabilization at long times, we infer that native state unfolding is negligible. Therefore, this process is not included in the kinetic scheme, and the folding time is equated to the first-passage time. Under these conditions, the kinetics of the system are described by the following sets of coupled linear equations:

For Scheme #1 (a single off-pathway kinetic trap)

$$\frac{dn_g}{dt} = r_{g,d}n_d - (r_{f,g} + r_{d,g})n_g \quad (1)$$

$$\frac{dn_d}{dt} = r_{d,g}n_g - r_{g,d}n_d \quad (2)$$

$$\frac{dn_f}{dt} = r_{f,g}n_g \quad (3)$$

For Scheme #2 (two off-pathway kinetic traps)

$$\frac{dn_g}{dt} = r_{g,d1}n_{d1} + r_{g,d2}n_{d2} - (r_{d1,g} + r_{d2,g} + r_{f,g})n_g \quad (4)$$

$$\frac{dn_{d1}}{dt} = r_{d1,g}n_g - r_{g,d1}n_{d1} \quad (5)$$

$$\frac{dn_{d2}}{dt} = r_{d2,g}n_g - r_{g,d2}n_{d2} \quad (6)$$

$$\frac{dn_f}{dt} = r_{f,g}n_g \quad (7)$$

For Scheme #3: (one off-pathway kinetic trap and one on-pathway intermediate)

$$\frac{dn_g}{dt} = r_{g,d}n_d + r_{g,i}n_i - (r_{d,g} + r_{i,g})n_g \quad (8)$$

$$\frac{dn_d}{dt} = r_{d,g}n_g - r_{g,d}n_d \quad (9)$$

$$\frac{dn_i}{dt} = r_{i,g}n_g - (r_{g,i} + r_{f,i})n_i \quad (10)$$

$$\frac{dn_f}{dt} = r_{f,i}n_i \quad (11)$$

Here $n_\alpha = n_\alpha(t)$ is the probability of finding the system in state α at time t, and $r_{\beta,\alpha}$ is the rate constant for transitions from state α to β. The systems of equations are solved, respectively, with the initial conditions $n_g(0) = 1$ and $n_d(0) = n_f(0) = 0$, $n_g(0) = 1$ and $n_{d1}(0) = n_{d2}(0) = n_f(0) = 0$, and $n_g(0) = 1$ and $n_d(0) = n_i(0) = n_f(0) = 0$. The population of the unfolded states is defined by the equations

$$n_{unfold}(t) = 1 - n_f(t) = n_g(t) + n_d(t) \quad (12)$$

$$n_{unfold}(t) = 1 - n_f(t) = n_g(t) + n_{d1}(t) + n_{d2}(t) \quad (13)$$

and

$$n_{unfold}(t) = 1 - n_f(t) = n_g(t) + n_d(t) + n_i(t) \quad (14)$$

for kinetic Schemes #1, #2, and #3, respectively, and the folding (first-passage) time distributions as

$$p_f(t) = \frac{dn_f(t)}{dt} \quad (15)$$

in all cases.

With the systems of eqs 1−2, 4−6, and 8−10 solved for the time-dependent populations of the corresponding states, eqs 12, 13, and 14 can be used to fit the required rate constants. For this, $n_{unfold}(t)$ values, given by eqs 12, 13, and 14, were compared with the experimental populations of the unfolded states. To fit the rate constants, we employed the maximum likelihood approach[13] with the mean-square functional. Although the solutions of the systems of eqs 1−2, 4−6, and 8−10 are readily written in an analytical form, we do not present them here. For Scheme #1 the solution of eqs 1−3 is a specific case of the solution of ref 12 for the infinitely large rate of collapse of the system, and for Schemes #2 and #3 they are Cardano's solutions[13] with all three roots real (the "trigonometric" form). These equations are of little use here because they are too complicated to reveal the dependence on the rate constants. In the latter two cases the roots of the characteristic equations were found numerically with use of Laguerre's method[14] and then verified with the Cardano solution. In all cases the solutions have the form

$$n_{unfold}(t) = \sum_{i=1}^{N} A_i \exp(-t/\tau) \quad (16)$$

Here $N = 1 + n_{int}$ is the number of the eigenvalues, where n_{int} is the number of off- and on-pathway intermediates and $A_i > 0$; for Scheme #1 $N = 2$, and for Schemes #2 and #3 $N = 3$.

III. Comparison with Experiment and Discussion

To estimate the rate constants, we used not original experimental points given in ref 4, which would require digitalization, but the multiexponential fits presented in the paper, which reproduce the original data very well. These fits are

$$0.82 \exp(-t/22\ \mu s) + 0.18 \exp(-t/5\ ms) \quad (T = 2\ °C) \quad (17)$$

and

$$0.38 \exp(-t/23\ \mu s) + 0.51 \exp(-t/261\ \mu s) + 0.11 \exp(-t/2\ ms) \quad (T = 8\ °C) \quad (18)$$

They are shown in Figures 2 and 3 by triangles and in Figure 4 by the solid line. The solid and dashed lines in Figure 2, the

TABLE 1: Ub*G Folding, $T = 2$ °C, Rate Constants $r_{\beta,\alpha}$ (μs^{-1}) and Waiting Times $\tau_{\beta,\alpha} = 1/r_{\beta,\alpha}$ (μs, in Parentheses)

	$r_{d,g}$ ($\tau_{d,g}$)	$r_{g,d}$ ($\tau_{g,d}$)			$r_{f,g}$ ($\tau_{f,g}$)
Scheme #1	8.1×10^{-3} (123)	2.4×10^{-4} (4106)			3.7×10^{-2} (27)
	$r_{d1,g}$ ($\tau_{d1,g}$)	$r_{g,d1}$ ($\tau_{g,d1}$)	$r_{d2,g}$ ($\tau_{d2,g}$)	$r_{g,d2}$ ($\tau_{g,d2}$)	$r_{f,g}$ ($\tau_{f,g}$)
Scheme #2	8.0×10^{-3} (125)	2.4×10^{-4} (4105)	4.1×10^{-9} (2.4×10^{9})	1.7×10^{-2} (60)	3.7×10^{-2} (27)

solid line in Figure 3, and the dashed line and triangles in Figure 4 present the corresponding analytical solutions, eqs 12−14 with the rate constants given in Tables 1, 3, and 5. Tables 2 and 4 compare theoretical characteristic times (τ_i) and preexponential factors (A_i) in eq 16 with those from eqs 17 and 18, respectively. The corresponding results for Scheme #3 are not shown, because no successful fit was obtained (Figure 4).

It is evident from Figure 3 that the single trap (off-pathway intermediate) and two traps (two off-pathway intermediates) give excellent fits to the experimental data. Introducing an additional off-pathway trap (d2 in Scheme #2) for $T = 2$ °C does not alter the result; i.e., the values of the rate constants obtained with Scheme #1 are essentially the same (Table 1), and the contribution of the exponential term responsible for this trap, which is determined by the preexponential factor A_2, is negligible (Table 2). Due to the latter the values of the rate constants $r_{d2,g}$ and $r_{g,d2}$ in Table 1 are not meaningful; variation of these constants does not affect the behavior of $n_{unfold}(t)$. Thus at $T = 2$ °C the presence of a single off-pathway trap is necessary and sufficient

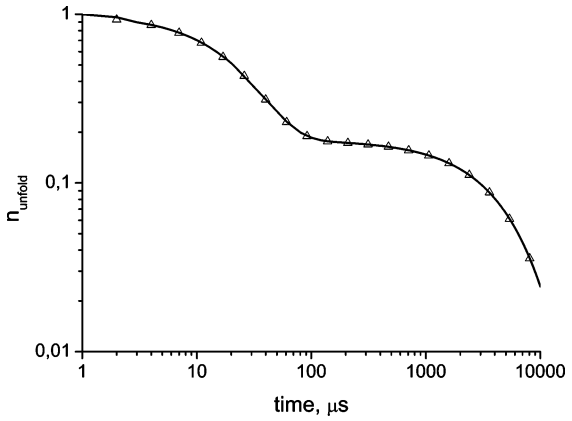

Figure 2. Population of the unfolded states of Ub*G at $T = 2$ °C. The triangles correspond to the experimental data of ref 4, and the solid and dashed lines, the difference between which is indistinguishable by eye, to the analytical solutions, eqs 12 and 13, with the rate constants from Table 1 for Schemes #1 and #2, respectively.

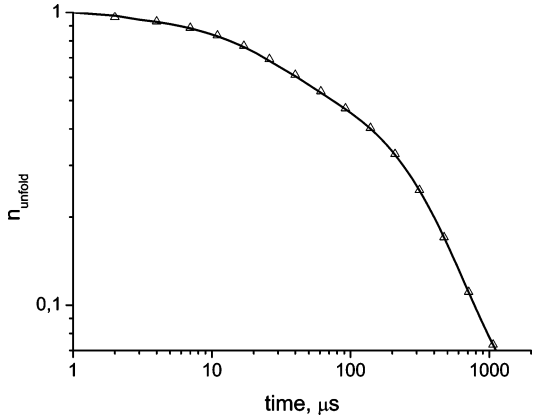

Figure 3. Population of the unfolded states of Ub*G at $T = 8$ °C. The triangles correspond to the experimental data of ref 4, and the solid line to the analytical solution, eq 13, with the rate constants from Table 3.

TABLE 2: Ub*G Folding, $T = 2$ °C, Multiple-Exponential Fit Parameters

	A_1	A_2	A_3	τ_1	τ_2	τ_3
Scheme #1	0.82		0.18	22		5002
Scheme #2	0.82	3.7×10^{-9}	0.18	22	60	5000
experiment	0.82		0.18	22		5000

to describe the folding process. According to ref 12, the double-exponential pattern of the kinetic curve demonstrates that the off-pathway trap is not in equilibrium with the semicompact globule; i.e., short folding times correspond to fast trajectories, which do not visit the off-pathway trap and go from the globule region to the native state directly, and long times correspond to slow trajectories, which visit the off-pathway trap, possible repeatedly, before reaching the native state. The fast trajectories are characterized by the time $\tau_{f,g} = 1/r_{f,g} \approx 27$ μs, which is close to the characteristic time of 22 μs in eq 17, and the slow trajectories by the time of order of $\tau_{g,d} = 1/r_{g,d} \approx 4.1$ ms, which is close to the other characteristic time, 5 ms, in eq 17. In the latter case the waiting times in the globule region, to pass into the trap ($\tau_{d,g} = 1/r_{d,g} \approx 123$ μs) and into the native state ($\tau_{f,g} = 1/r_{f,g} \approx 27$ μs), are negligible in comparison with that to leave the trap, $\tau_{g,d} \approx 4.1$ ms.

Since the kinetic curve contains three exponential terms, eq 18, at $T = 8$ °C a second intermediate contributes. Figures 3 and 4 show the best fits obtained with Schemes #2 (an additional off-pathway trap) and #3 (an additional on-pathway intermediate), respectively. Figure 4 also depicts the best fit obtained with Scheme #1 (no additional intermediate). As follows from these figures, an additional intermediate is required, and it must be an off-pathway trap, given our models. This is supplemented by the fact that for Scheme #2 none of the exponential terms in eq 16 is negligible (i.e., A_1, A_2, and A_3 in Table 4), while the values of the rate constants are meaningful and differ considerably (Table 3). Both traps, d1 and d2, are not in equilibrium with the semicompact globule, as in the case for the one

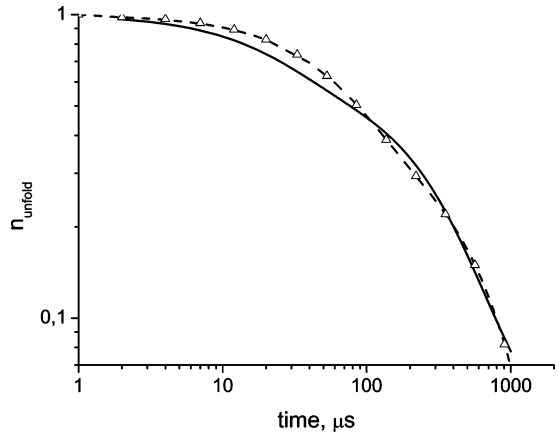

Figure 4. Population of the unfolded states of Ub*G at $T = 8$ °C. The solid line corresponds to the experimental data of ref 4, the triangles to the best fit obtained with kinetic Scheme #3, eq 14, and the dashed line to that obtained with kinetic Scheme #1, eq 12; as can be seen from the figure, the latter two yield essentially identical results. The corresponding rate constants for the given analytical solutions are presented in Table 5.

TABLE 3: Ub*G Folding, $T = 8$ °C, Rate Constants $r_{\beta,\alpha}$ (μs^{-1}) and Waiting Times $\tau_{\beta,\alpha} = 1/r_{\beta,\alpha}$ (μs, in Parentheses)

	$r_{d1,g}$ ($\tau_{d1,g}$)	$r_{g,d1}$ ($\tau_{g,d1}$)	$r_{d2,g}$ ($\tau_{d2,g}$)	$r_{g,d2}$ ($\tau_{g,d2}$)	$r_{f,g}$ ($\tau_{f,g}$)
Scheme #2	2.0×10^{-3} (510)	5.6×10^{-4} (1799)	2.0×10^{-2} (51)	8.0×10^{-3} (125)	1.9×10^{-2} (52)

TABLE 4: Ub*G Folding, $T = 8$ °C, Three-Exponential Fit Parameters

	A_1	A_2	A_3	τ_1	τ_2	τ_3
Scheme #2	0.38	0.51	0.11	22	262	2000
experiment	0.38	0.51	0.11	23	261	>2000

intermediate at $T = 2$ °C. If either trap were in equilibrium with the globule, then it would form an "extended" globule,[12] and Scheme #1 would be applicable, which does not fit the data (Figure 4).

Generalization of the expression for the mean folding time, derived in ref 12 for Scheme #1, gives

$$\bar{t}_f = \frac{1}{r_{f,g}}\left(1 + \sum_{k=1}^{n_d} \frac{r_{dk,g}}{r_{g,dk}}\right) \tag{19}$$

where n_d is the number of off-pathway traps. From this equation follows that though trap d2 is much more shallow than d1 (their waiting times are related as $125/1799 \approx 0.07$), its contribution to the mean folding time is of the same order ($2.0 \times 10^{-2}/8.0 \times 10^{-3} \approx 2.5$ for d2 against $2.0 \times 10^{-3}/5.6 \times 10^{-4} \approx 3.5$ for d1). This is because the shorter waiting time of the system in trap d2 is approximately compensated for by more frequent visits to it (Table 3).

With the rate constants of Tables 1 and 3, eq 19 gives for $T = 2$ °C and $T = 8$ °C, $\bar{t}_f \approx 930$ μs and $\bar{t}_f \approx 365$ μs, respectively. Direct calculation of the mean folding times

$$\bar{t}_f = \int_{t_{min}}^{t_{max}} t p_f(t)\, dt$$

where the folding time distributions $p_f(t)$ (eq 15) are found by differentiation of eqs 17 and 18. The values are $\bar{t}_f \approx 970$ μs and $\bar{t}_f \approx 370$ μs for $T = 2$ °C and $T = 8$ °C, respectively; $t_{min} = 1$ μs, and t_{max} was chosen to be as large as 10^3 ms. It is of interest that the decrease of the mean folding time with temperature is not due to the increase of the rate constant for the transition from the semicompact globule to the native state ($r_{f,g}$). As eq 19 and Tables 1 and 3 show, $\bar{t}_f$ decreases because the effect of the two traps at $T = 8$ °C is much smaller ($r_{d1,g}/r_{g,d1} + r_{d2,g}/r_{g,d2} \approx 6$) than that of the single trap at $T = 2$ °C ($r_{d,g}/r_{g,d} \approx 33$).

The eigenvalues of the system of kinetic equations (i.e., τ_i in eq 16) do not generally represent waiting times in specific states but are instead complex functions of the full set of rate constants (see, e.g., ref 12). However, in some cases such a correspondence does exist, as for example at $T = 2$ °C, where $\tau_1 \approx 22$ μs is close to the waiting time to pass from the globule to the native state ($\tau_{f,g} \approx 27$ μs); also $\tau_2 \approx 5$ ms is close to the time associated with the visits to the trap ($\tau_{d,g} + \tau_{g,d} \approx 4.2$ ms). At $T = 8$ °C the situation is not so simple because here two traps exist and the correspondence between the eigenvalues and the waiting times is more complex.

For Scheme #3, which presents a combination of off-pathway and on-pathway traps (Figure 1), no successful fit has been obtained at $T = 8$ °C. The closest one, among various attempts, is shown in Figure 4 by triangles, with the corresponding values of rate constants given in Table 5. It is of interest that this curve practically coincides with the best fit obtained for this temperature with Scheme #1 (the dashed line in Figure 4), in which case only two exponential terms are present (Table 5). This is because the on-pathway intermediate is in equilibrium with the semicompact globule, forming an "extended globule". Indeed, as one can see from Table 5, transitions between the globule and the intermediate are very fast in comparison with the others, so that detailed balance between the globule and the intermediate holds approximately; i.e., $r_{g,i}n_i \approx r_{i,g}n_g$. Introducing the population of the extended globule $\tilde{n}_g = n_g + n_i \approx (1 + r_{i,g}/r_{g,i})n_g = (1 + r_{g,i}/r_{i,g})n_i$ and summing up eqs 8 and 10, one obtains

$$\frac{d\tilde{n}_g}{dt} = r_{g,d}n_d - (\tilde{r}_{f,g} + \tilde{r}_{d,g})\tilde{n}_g \tag{20}$$

where $\tilde{r}_{d,g} = r_{d,g}r_{g,i}/(r_{i,g} + r_{g,i})$ and $\tilde{r}_{f,g} = r_{f,i}r_{i,g}/(r_{i,g} + r_{g,i})$. Correspondingly, eqs 9 and 11 can be rewritten as

$$\frac{dn_d}{dt} = \tilde{r}_{d,g}\tilde{n}_g - r_{g,d}n_d \tag{21}$$

$$\frac{dn_f}{dt} = \tilde{r}_{f,g}\tilde{n}_g \tag{22}$$

The system of eqs 20−22 is completely equivalent to that for Scheme #1, eqs 1−3, and thus leads to the same distribution of folding times. This is confirmed by the values of rate constants given in Table 5; the constant $r_{g,d}$, which was not altered by the transformations, does not change. For $\tilde{r}_{d,g}$ and $\tilde{r}_{f,g}$ for the extended globule, we have $\tilde{r}_{d,g} \approx 4.7 \times 10^{-3}$ μs and $\tilde{r}_{f,g} \approx 1 \times 10^{-2}$ μs, which coincide with the values of $r_{d,g}$ and $r_{f,g}$ for Scheme #1, respectively (Table 5).

With a knowledge of the forward and backward rate constants (Tables 1 and 3), it is possible to calculate the free energies of the off-pathway traps with respect to the globule. Assuming detailed balance, $r_{j,i}/r_{i,j} = \exp[-(F_j - F_i)/k_BT]$, where F_α is the free energy of state α and k_B is the Boltzmann constant, we have $F_{d1} - F_g \approx -1.9$ and $F_{d2} - F_g \approx 9.6$ at $T = 2$ °C, and $F_{d1} - F_g \approx -0.7$ and $F_{d2} - F_g \approx -0.5$ at $T = 8$ °C, with the energy measured in kcal/mol. An additional assumption about the value of the prefactor $A_{j,i}$ in the Arrhenius equation, $r_{j,i} = A_{j,i}\exp(-\Delta F_{j,i}/k_BT)$, makes it possible to estimate tentative values of the effective free energy barriers between the states, $\Delta F_{j,i}$. For this, we assume that the $A_{j,i}$ values are equal to the frequently used "speed limit" of 1 μs^{-1}, characteristic of small proteins (consisting of approximately 100 residues or less),[15] although this assumption is, strictly speaking, applicable only to the transitions from the globule to the native state (the last

TABLE 5: Ub*G Folding, $T = 8$ °C, Rate Constants $r_{\beta,\alpha}$ (μs^{-1}) and Waiting Times $\tau_{\beta,\alpha} = 1/r_{\beta,\alpha}$ (μs, in Parentheses)

	$r_{d,g}$ ($\tau_{d,g}$)	$r_{g,d}$ ($\tau_{g,d}$)	$r_{i,g}$ ($\tau_{i,g}$)	$r_{g,i}$ ($\tau_{g,i}$)	$r_{f,i}$ ($\tau_{f,i}$)
Scheme #3	9.7×10^{-3} (103)	2.7×10^{-3} (370)	1.0 (1)	9.4×10^{-1} (1.1)	2.0×10^{-2} (50)

	$r_{d,g}$ ($\tau_{d,g}$)	$r_{g,d}$ ($\tau_{g,d}$)	$r_{f,g}$ ($\tau_{f,g}$)
Scheme #1	4.7×10^{-3} (213)	2.7×10^{-3} (370)	1.0×10^{-2} (100)

TABLE 6: Ub*G Folding: Effective Free Energy Barriers between the Characteristic States (kcal/mol)

	$\Delta F_{d1,g}$	$\Delta F_{g,d1}$	$\Delta F_{d2,g}$	$\Delta F_{g,d2}$	$\Delta F_{f,g,}$
$T = 2$ °C	2.6	4.6	11.8	2.2	1.8
$T = 8$ °C	3.5	4.2	2.2	2.7	2.2

column of Table 6). The results are shown in Table 6, and they are similar in magnitude to the free energy barriers obtained for a set of small proteins in ref 15. Of course, the actual value of the barrier depends on the choice of the preexponential factor. The observed large variation of the effective free energies with temperature is indicative of the complexity of the system and the temperature dependence of the reduced energy landscape.

IV. Conclusion

Sabelko et al.[4] suggested that at $T = 8$ °C the folding kinetics of a ubiquitin mutant follows a downhill folding scenario, which resulted in a stretched-exponential distribution of unfolded states, while at $T = 2$ °C, two-exponential behavior is observed. However, they also showed that the kinetic curve at $T = 8$ °C is well fitted by a three-exponential distribution. In this paper, we have introduced a simple kinetic model that describes the experimental data. It is based on lattice model studies and includes a semicompact globule, off- and on-pathway intermediates, and the native state as possible contributing states. Three kinetics schemes were examined, which differ from each other by the intermediates involved: one off-pathway trap (Scheme #1), two off-pathway traps (Scheme #2), and one off-pathway and one on-pathway traps (Scheme #3). Comparing the theoretical solutions with the experimental results, we have estimated both the rate constants determining the transitions between the states of the system and the relative free energies of the states. The observed large variation of the effective free energies with temperature is indicative of the complexity of the system and the temperature dependence of the reduced energy landscape. Both the low- and the high-temperature experiments (i.e., at $T = 2$ °C and $T = 8$ °C) are well-described within the framework of Scheme #2. However, at low temperature ($T = 2$ °C) only one trap is essential, and Scheme #2 reduces to Scheme #1. In accord with the variation of the free energy surface with temperature, which was proposed for ubiquitin (see Figure 6 in ref 4), it is possible that the cold- and heat-denaturated states of Ub*G are involved in the off-pathway traps. If so, when one passes from $T = 2$ °C, where cold denaturation dominates, to $T = 8$ °C, which corresponds to the optimum native stability,[4] the role of the cold-denaturated state in the folding process would decrease and that of the heat denaturated state would increase. Alternatively, a trap could be associated with a state having excess helix relative to the native state.[16] We hope the present analysis will stimulate further studies of ubiquitin, a model system for which a definitive folding mechanism is likely to be determined by additional experimental and theoretical analyses.

Acknowledgment. We thank M. Gruebele for helpful comments and P. Maragakis for useful discussion. This work was supported in part by a grant from the CRDF (RUP2-2629-NO-04). The research at Harvard was supported in part by a grant from the National Institutes of Health. S.F.C. also acknowledges support from the RFBR (#06-04-48587).

References and Notes

(1) Ferguson, N.; Fersht, A. R. *Curr. Opin. Struct. Biol.* **2003**, *13*, 75−81.
(2) Went, H. M.; Benitez-Cardoza, C. G.; Jackson, S. E. *FEBS Lett.* **2004**, *567*, 333−338.
(3) Khorasanizadeh, S.; Peters, I. D.; Butt, T. R.; Roder, H. *Biochemistry* **1993**, *32*, 7054−7063.
(4) Sabelko, J.; Ervin, J.; Gruebele, M. *Proc. Natl. Acad. Sci. U.S.A.* **1999**, *96*, 6031−6036.
(5) Bryngelson, J. D.; Wolynes, P. G. *Proc. Natl. Acad. Sci. U.S.A.* **1987**, *84*, 7524−7528.
(6) Dinner, A.; Šali, A.; Karplus, M.; Shakhnovich, E. *J. Chem. Phys.* **1994**, *101*, 1444−1451.
(7) Shlesinger, M. F.; Zaslavsky, G. M.; Klafter, J. *Nature* **1993**, *363*, 31−37.
(8) Nymeyer, H.; García, A. E.; Onuchic, J. N. *Proc. Natl. Acad. Sci. U.S.A.* **1998**, *95*, 5921−5928.
(9) Skorobogatiy, M.; Guo, H.; Zuckermann, M. *J. Chem. Phys.* **1998**, *109*, 2528−2535.
(10) Metzler, R.; Klafter, J.; Jortner, J.; Volk, M. *Chem. Phys. Lett.* **1998**, *293*, 477−484.
(11) Sorenson, J. M.; Head-Gordon, T. *Proteins: Struct., Funct., Genet.* **2002**, *46*, 368−379.
(12) Chekmarev, S. F.; Krivov, S. V.; Karplus, M. *J. Phys. Chem. B* **2005**, *109*, 5312−5330.
(13) Korn, G. A.; Korn T. M. *Mathematical Handbook for Scientists and Engineers*, 2nd ed.; McGraw-Hill: New York, 1968.
(14) Press: W. H.; Flannery, B. P.; Teukolsky, S. A.; Vetterling, W. T. *Numerical Recipes in Fortran*; 2nd ed.; Cambridge University Press: Cambridge, U. K., 1992.
(15) Kubelka, J.; Hofrichter, J.; Eaton, W. A. *Curr. Opin. Struct. Biol.* **2004**, *14*, 76−88.
(16) Gruebele, M. University of Illinois at Urbana−Champaign, Urbana, IL. Personal communication.